

Search for correlations between high-energy gamma rays and neutrinos with the HAWC and ANTARES detectors

G. Ferrara^{a,*} and L. Fusco^b on behalf of the ANTARES and HAWC Collaboration
(a complete list of authors can be found at the end of the proceedings)

^a*INFN-LNS, Via S. Sofia 62, Catania, Italy*

^b*Aix Marseille Univ, CNRS/IN2P3, CPPM, Marseille, France*

E-mail: gferrara@lns.infn.it, fusco@cppm.in2p3.fr

ANTARES is an underwater neutrino detector in the Mediterranean Sea. Its location, reconstruction accuracy for all-flavor neutrino interactions, and low energy threshold, make it the most sensitive neutrino observatory for searches below 100 TeV over large parts of the sky. The HAWC experiment is a water Cherenkov gamma-ray detector located in Mexico. Thanks to its large field of view it is an excellent instrument to observe the very-high energy gamma-ray sky and perform high-sensitivity surveys of the Galactic Plane. The 10-year ANTARES data set and 3-year HAWC point source surveys are used to search for all-flavor neutrino emission in correlation with the highly-significant observations by HAWC in the gamma-ray sky by means of a maximum-likelihood template search. No significant observation for a correlation has been identified and upper limits on the neutrino flux from the HAWC observations have been set.

37th International Cosmic Ray Conference (ICRC 2021)
July 12th – 23rd, 2021
Online – Berlin, Germany

*Presenter

1. Introduction

The search for the origin of Galactic Cosmic Rays (GCRs) led to consider most of the sources located in the Galactic Plane responsible for the acceleration of GCRs up to PeV energies. The very-high-energy observations of these point-like sources give us the possibility to study GCR accelerators and the mechanisms responsible for their acceleration.

The interaction of the hadronic component of GCRs with the dense inter-stellar medium (ISM), either close to the sources or while they diffuse through the Galactic Plane (GP), is expected to produce high-energy photons and neutrinos via the decay chains of neutral and charged mesons, carrying roughly 5 and 10% of the primary CRs energy, respectively [5]. GCRs around the *knee* of the energy spectrum would thus produce neutrinos and photons mostly at energies of about 10–100 TeV [6]. On the other hand, the interaction of the leptonic component of primary CRs are expected to produce only photons via radiative energy loss processes.

Multi-messenger searches combining gamma-ray and neutrino observations are necessary for the better understanding of Galactic accelerators. In order to disentangle the hadronic and leptonic scenarios, and enhance the identification of an individual Cosmic Rays (CR) accelerator, the association between high-energy neutrinos¹ and high-energy gamma-rays should be investigated.

Surveys of GP gamma-ray emitters are available from data collected by the H.E.S.S. (High Energy Stereoscopic System)[7] and HAWC (High-Altitude Water Cherenkov) Observatory [9, 11, 12]. Supernova Remnants (SNRs) and Pulsar Wind Nebula (PWNe) constitute the majority of identified sources, even though a large quantity of high-energy emission has not yet been classified as belonging to a specific class of objects. The H.E.S.S. high-energy observation of the very central part of our Galaxy suggests the presence of PeV CRs interacting with the local medium [14].

Both the ANTARES [15] and IceCube [16] Collaborations put upper limits on neutrino emissions from point-like and extended sources in the central part of the GP, with the best results coming from the combination of the data samples collected by both experiments [17] – no significant excess of cosmic events above the atmospheric foregrounds is observed. Similarly, searches are conducted aiming at the identification of the diffuse component produced by GCR interaction with the ISM, both by ANTARES [18, 19] and IceCube [20] and a combination of their data samples [21]. Moreover no Galactic neutrino emitter or emission region is identified.

In this work, data collected with the ANTARES neutrino telescope and with the HAWC observatory are used to probe a possible correlation between high-energy gamma-rays and neutrinos.

2. The ANTARES and HAWC detectors

The HAWC observatory [23] is a high-energy gamma-ray detector, located at an altitude of 4100 meters above sea level, on the flanks of the Sierra Negra volcano near Puebla, Mexico. The detector is composed of 300 cylindrical water tanks, 4.5 meter high and 7.3 meter in diameter [24]. Each tank is equipped with four photomultiplier tubes (PMTs), the central one is 10 inches, while the 3 peripheral are 8 inches, located at the bottom of the tank. The PMTs collect the Cherenkov light induced in the water contained in the tank by particles produced by the interaction of gamma-rays and CRs in the atmosphere [27, 28].

¹Here and in the following, the word *neutrino* refers to both ν and $\bar{\nu}$ unless otherwise specified.

The HAWC configuration allows the detector to be sensitive to gamma-rays in the energy range between ~ 300 GeV up to a few hundred TeV, and to reach an angular resolution between 0.1 and 1 degree. The full detector has been operational since March 2015, continuously observing the sky with an instantaneous field of view of 15% of the sky and covering daily two thirds of the sky, with high duty cycle within the declination range from -26° to 64° .

The ANTARES telescope [25] is an underwater neutrino detector - anchored to the seabed at a depth of about 2500 metres, off-shore the southern coast of France. The detector consists of a three-dimensional array of 885 optical modules (OMs) distributed over 12 450-m long vertical strings and arranged on a 140-m wide footprint, with a instrumented volume of 0.02 km^3 . Each OM is a pressure-resistant glass sphere hosting a 10-inch PMT.

Detector operations began in 2007 and the apparatus is taking data continuously in its full configuration since 2008. With an instantaneous field-of-view of more than 2π - by observing upward-going particles passing through the Earth from below the detector - the detector allows for almost complete daily coverage of the sky at energies between 100 GeV and 1 PeV, with a median angular resolution of the order of 0.4° [29].

3. Data analysis

In the analysis presented here, the data samples collected by the HAWC Observatory while performing two sky surveys for the search for point sources are used. The first sample, named *sample A*, consists of data collected from November 2014 to June 2019 [11] in the energy range between 300 GeV up to few hundred TeV. A second sample, hereinafter referred to as *sample B*, comprises events with a measured shower energy above a threshold of 56 TeV collected from June 2015 to June 2019. As a result of the HAWC analysis of such data samples, sky-maps providing the value of the differential gamma-ray fluxes in each point of the sky are obtained under a point-source emission hypothesis and following the assumption that the energy spectrum of the gamma-ray emission is described by an unbroken power-law $d\Phi/dE \propto E^{-\Gamma}$ with a fixed spectral index Γ and pivot energy of 7 TeV. For *sample A*, whose energy spectrum covers the full energy range of sensitivity of the HAWC detector, a spectral index $\Gamma = 2.5$ is assumed, while for *sample B*, consisting of only high energy events, a harder spectrum with $\Gamma = 2.0$ is considered, as in [12]. The significance of the detection of gamma-ray sources is then given as the sky-map of square root of the test statistic (\sqrt{TS} in the following) of the point-source searches.

To reduce the contribution of unresolved sources and prevent the overestimation of the possible neutrino flux, in the analysis presented here a highly-significant observation of gamma-ray sources is required. In order to achieve such condition a \sqrt{TS} cut corresponding to a 3σ Gaussian significance is applied on the test statistic sky-maps of both *sample A* and *sample B*. In addition to this, the declination range of the search is restricted to $[-20^\circ, 60^\circ]$ in order to remove sky regions to which the HAWC detector is less sensitive. Figure 1 shows the sky maps of the differential gamma-ray flux, in galactic coordinates, of the two data samples. For *sample B* a zoom of the galactic plane region with galactic latitude $b \in [-3^\circ, 3^\circ]$ is shown.

The ANTARES data sample acquired between February 2007 and December 2017 is used in this work, following the same event selection as in the ANTARES point-source search described in [29]. Track-like events (*tr*), induced by charged current muon neutrino interactions [30], and shower-

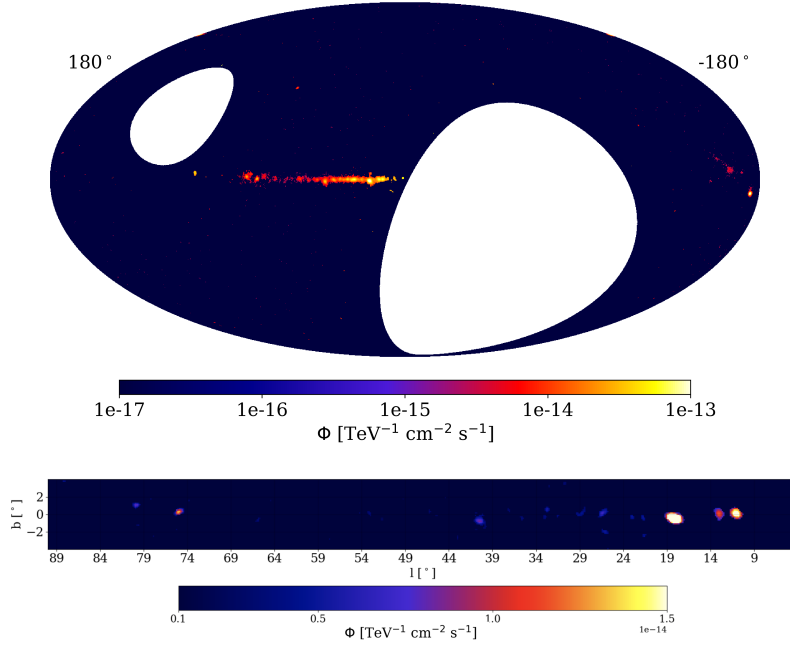


Figure 1: Sky-maps of the HAWC differential flux, for *sample A* (upper panel) and *sample B* (lower panel). The maps are obtained applying a cut corresponding to 3σ on the value of the square root of the HAWC test statistic distributions. The maps are reported in the galactic coordinate reference system.

like events (*sh*), produced by all neutrino flavours and all interaction channels [31], are selected. The background given by downward-going atmospheric muons arriving at large depths is largely reduced by means of selection cuts based on the quality parameters provided by the reconstruction algorithms. According to Monte Carlo (MC) simulations [32], a residual contamination from background of 10% of the sample survives the cuts.

The HAWC sky-maps obtained from *sample A* and *B* are used as spatial and energy templates for a likelihood-based search for astrophysical neutrino candidates in the ANTARES sample. In particular, the same analysis strategy followed in the ANTARES search for Galactic diffuse neutrino flux [19] is applied. The neutrino flux is evaluated from the observed gamma-ray spectrum detected by HAWC according to the model and the assumptions of *Villante and Vissani* [22], and considering equipartition between the three neutrino flavours as expected from standard neutrino emission scenarios and neutrino oscillations over cosmic distances [6].

To evaluate the significance of the association between gamma-rays and cosmic neutrinos in the ANTARES data sample dominated by atmospheric events, a test statistic Q is built as:

$$Q = \log \mathcal{L}_{\text{sig} + \text{bkg}} - \log \mathcal{L}_{\text{bkg}} \quad (1)$$

The likelihood function $\mathcal{L}_{\text{sig} + \text{bkg}}$ is defined as follows:

$$\mathcal{L}_{\text{sig} + \text{bkg}} = \prod_{\text{evt} \in \{\text{tr}, \text{sh}\}} \prod_{i \in \text{evt}} \left[\mu_{\text{sig}}^{\text{evt}} \cdot pdf_{\text{sig}}^{\text{evt}}(E_i, \alpha_i, \delta_i) + \mu_{\text{bkg}}^{\text{evt}} \cdot pdf_{\text{bkg}}^{\text{evt}}(E_i, \delta_i) \right] \quad (2)$$

where product sequences are over the event topology *evt* (track-like and shower-like neutrino events) and over each event *i* belonging to the sample *evt*. The E_i is the reconstructed energy, α_i and δ_i

are the right ascension and declination of the event. The $\mu_{\text{sig}}^{\text{evt}}$ parameter is the number of signal events which maximizes the likelihood function while $\mu_{\text{bkg}}^{\text{evt}}$ is the number of background events in the sample.

The signal and background probability density functions (PDFs), $pdf_{\text{sig}}^{\text{evt}}$ and $pdf_{\text{bkg}}^{\text{evt}}$, are defined as the product of two contributions: a spatial component, which encloses the information of the arrival direction of the ANTARES neutrino events, and an energy term describing the expected energy spectrum of the signal and background components.

For the signal, the spatial term depends on the equatorial coordinates of the events (α_i, δ_i). It is given by the expected arrival direction of the reconstructed neutrino events produced in a dedicated MC simulation of the ANTARES response. In the case of background the PDF is derived by computing spline-fits of the δ_i distribution of selected neutrino data set, which allows even to account for possible statistical fluctuations in the event sample.

Both for signal and background, the energy term accounts for the energy spectrum of the reference model used to describe the spectral features of the event sample. In the case of signal the energy spectra of the reference model of neutrino signal is used. While for the background the *Honda et al.* model [33] is considered. The energy term is then built as the distribution of the energy estimator of reconstructed events as a function of the reconstructed declination of the event, obtained in the full MC simulation of the detector.

The test statistic Q distributions are then built by means of pseudo-experiments (PE). A total of 10^3 pseudo-experiments are performed, in which the search method is applied to pseudo data-sets by varying the number of signal events $\mu_{\text{sig}}^{\text{evt}} = \mu_{\text{sig}}^{\text{tr}} + \mu_{\text{sig}}^{\text{sh}}$ injected in the neutrino sample, from 0 up to 30 with 1 event step, and randomly scrambling the background events. The probability density functions of Q , $pdf(Q)$, are then used to estimate the median sensitivity at 90% confidence level (c.l.). The statistical and systematical uncertainties due to the detector response is here treated as in [29]. Example of the $pdf(Q)$ distributions are reported in the left panel of Figure 2.

4. Results and conclusions

The search method based on the maximum likelihood approach described above is used to compute the best-fit value for the number of signal events $\mu_{\text{sig}}^{\text{tr}+sh}$ in the ANTARES unscrambled data set. In order to estimate the significance of the observation a p -value is computed by comparing the obtained value of the test statistic, Q_{obs} , with the distribution of Q for the background-only hypothesis obtained from scrambled pseudo data-sets. The p -value is then represented by the percentage of the PEs with a value of the test statistic Q higher than Q_{obs} . Finally, following the same approach described in [35], the 90% c.l. upper limit (u.l.) on the maximal number of signal events ($\text{tr}+sh$) $\mu_{\text{sig}}^{\text{u.l.}}$ is obtained.

The corresponding upper limit on the number of signal events, $n_{\text{sig}}^{\text{u.l.}}$, and the ratio to the number of signal events n_{sig}^0 expected from the assumed model of neutrino emission is reported in Table 1 both for *sample A* and *sample B*, together with the energy range of validity of these limits, computed as the region of the signal neutrino spectrum where the central 90% of events would be visible in ANTARES.

The u.l. on the number of events are translated into differential flux limits, $\Phi_{\nu}^{\text{u.l.}}$, being $\Phi_{\nu}^{\text{u.l.}} = n_{\text{sig}}^{\text{u.l.}} / n_{\text{sig}}^0 \cdot \Phi_{\nu}^{A,B}$, where $\Phi_{\nu}^{A,B}$ is the cumulative differential neutrino flux averaged over the solid

| HAWC Sky-map | μ_{sig}^{tr} | μ_{sig}^{sh} | p-value | $n_{\text{sig}}^{\text{u.l.}}$ | n_{sig}^0 | $\frac{n_{\text{sig}}^{\text{u.l.}}}{n_{\text{sig}}^0}$ | ΔE [TeV] |
|-----------------|-------------------------|-------------------------|---------|--------------------------------|--------------------|---|------------------|
| <i>sample A</i> | 6.4 | 0 | 0.18 | 9.6 | 1.5 | 6.5 | 0.45 - 56.2 |
| <i>sample B</i> | 0 | 0 | 0.33 | 5.0 | 1.0 | 4.9 | 1.78 - 89.1 |

Table 1: A summary of the analysis results is reported. For each of the HAWC sky-map the fitted number of signal tracks and showers, the corresponding p-value, the u.l. at 90 c.l. on the number of signal events, the expected signal from the model described in the text, as well as their ratio are shown. In the last column the energy range containing the 90% of reconstructed signal event is also indicated.

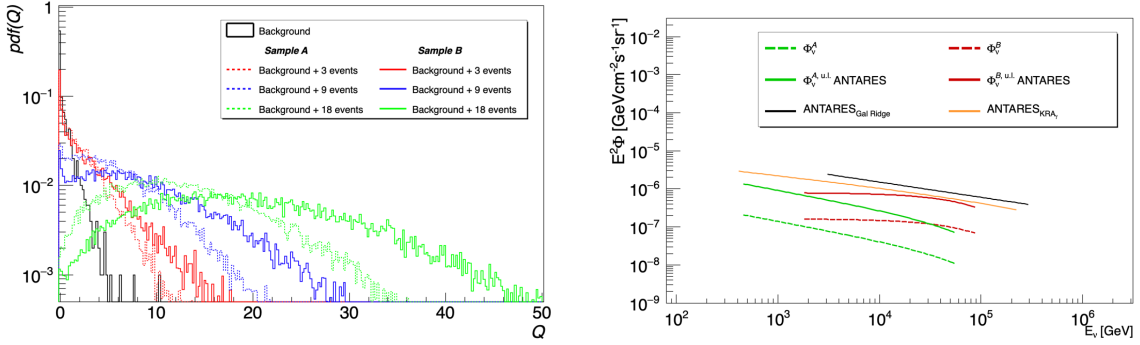


Figure 2: In the left panel the distributions of the probability density function $pdf(Q)$ of the test statistic for the background-only case, and for $\mu_{\text{sig}} = 3, 9$ and 18 for *sample A* and *sample B* are shown. In the right panel the differential flux upper limits for *sample A* (green solid line) and for *sample B* (red solid line) are shown. These limits are compared to the expectations (green/red dashed lines) with the models used in these analyses and with previous ANTARES results in the same area of the sky [18, 19].

angle covered by *sample A* and *sample B*. In the right panel of Figure 2 the u.l. on differential fluxes are compared to the reference neutrino signal assumed in this analysis, derived from the gamma-ray spectrum of the HAWC point-source sky maps according to [22], and with previous ANTARES results obtained from dedicated diffuse Galactic emission searches in the same area of the sky [18, 19].

The ANTARES result from this work is compatible with a non-observation of neutrino emissions spatially coincident with the HAWC signal, expected in case of hadronic production of gamma-rays. This result is valid for both the two different spectral assumptions of the HAWC gamma-ray flux. The sensitivity of ANTARES is still a factor ~ 5 (refer to Table 1) above the neutrino prediction computed from the gamma-ray flux with the two spectral assumptions and the upper limits derived from this search are compatible with what could be expected from the sensitivity level of the analyzed neutrino data-set.

References

- [1] V. Ptuskin, V. Zirakashvili and E.-S. Seo, *Astrophys. Journ.* **718**, 1 (2010)
- [2] W. Bednarek and M. Bartosik, *Astron. and Astrophys.* **423**, 405 (2004)
- [3] S. Heinz and R. Sunyaev, *Astron. and Astrophys.* **390**, 751 (2002)
- [4] K. Kotera and A. V. Olinto, *The Astrophysics of Ultrahigh Energy Cosmic Rays*, in *Ann. Rev. Astron. and Astrophys.* **49**, 119-153 (2011)
- [5] S.R. Kelner and F.A. Aharonian, *Phys. Rev. D* **78**, 034013 (2008) [Erratum: *Phys. Rev.D* **82**,099901 (2010)]
- [6] T. K. Gaisser, R. Engel and E. Resconi, *Cosmic Rays and Particle Physics*, Cambridge University Press (2016). doi:10.1017/CBO9781139192194
- [7] H. Abdalla et al., *Astron. and Astrophys.* **612**, A1 (2018)
- [8] A. Albert et al., *Astrophys. Journ. Lett.* **868**, L20 (2018)
- [9] A. U. Abeysekara et al., *Astrophys. J.* **843**, 40 (2017)
- [10] A.U. Abeysekara et al., *Astrophys. Journ.* **881**, 134 (2019)
- [11] A. Albert et al., *Astrophys. J.* **905**, 76 (2020)
- [12] A.U. Abeysekara et al., *Phys. Rev. Lett.* **124**, 021102 (2020)
- [13] H. Abdalla et al., *Astron. and Astrophys* **612**, A6 (2018)
- [14] A. Abramowski et al., *Nature* **531**, 476 (2016)
- [15] A. Albert et al., *Phys. Rev. D* **96**, 082001 (2017)
- [16] M.G. Aartsen et al., *Eur. Phys. J. C* **79**, 234 (2019)
- [17] A. Albert et al., *Astrophys. Journ.* **892**, 92 (2020)
- [18] S. Adrián-Martínez et al., *Phys. Lett. B* **760**, 143 (2016)
- [19] A. Albert et al., *Phys. Rev. D* **96**, 062001 (2017)
- [20] M.G. Aartsen et al., *Astrophys.J.* **849**, 67 (2017)
- [21] A. Albert et al., *Astrophys. Journ. Lett.* **868**, L2 (2018)
- [22] F.L. Villante and F. Vissani, *Phys. Rev. D* **78**, 103007 (2008)
- [23] A. U. Abeysekara et al., *Nucl. Instrum. Methods Phys. Res. Sec. A* **888**. 138 (2018)
- [24] A.U. Abeysekara et al., *Astroparticle Physics* **62**, 125–133 (2015)

- [25] M. Ageron et al., Nucl. Instrum. Methods Phys. Res., Sect. A **656**, 11 (2011)
- [26] S. Adrián-Martínez et al., J. Phys. G: Nucl. Part. Phys. **43**, 084001 (2016)
- [27] A. U. Abeysekara et al., Astrophys. J. **843**, 39 (2017)
- [28] Andrew J. Smith for the HAWC Collaboration, *HAWC: Design, Operation, Reconstruction and Analysis*, **PoS(ICRC2015)966**
- [29] A. Albert et al., Phys. Rev. D **96**, 082001 (2017)
- [30] S. Adrian-Martinez et al., Astrophys. Journ. **760**, 53 (2012)
- [31] A. Albert et al., Astronom. Journ. **154**, 6 (2017)
- [32] A. Albert et al., accepted for publication by Journ. Cosm. Astrop. Phys. arxiv2010.06621
- [33] M. Honda et al. Phys. Rev. D 75: 043006, 2007
- [34] S. Aiello et al., Astroparticle Physics **111**, 110 (2019)
- [35] J.J. Neyman, Phil. Trans. Roy. Soc. Lond. A **236** no. 767, 333 (1937)

Full Authors List: ANTARES Collaboration

A. Albert^{1,2}, S. Alves³, M. André⁴, M. Anghinolfi⁵, G. Anton⁶, M. Ardid⁷, S. Ardid⁷, J.-J. Aubert⁸, J. Aublin⁹, B. Baret⁹, S. Basa¹⁰, B. Belhorma¹¹, M. Bendahman^{9,12}, V. Bertin⁸, S. Biagi¹³, M. Bissinger⁶, J. Boumaaza¹², M. Bouta¹⁴, M.C. Bouwhuis¹⁵, H. Brânzaș¹⁶, R. Bruijn^{15,17}, J. Brunner⁸, J. Busto⁸, B. Caiffi⁵, A. Capone^{18,19}, L. Caramete¹⁶, J. Carr⁸, V. Carretero³, S. Celli^{18,19}, M. Chabab²⁰, T. N. Chau⁹, R. Cherkaoui El Moursli¹², T. Chiarusi²¹, M. Circella²², A. Coleiro⁹, M. Colomer-Molla^{9,3}, R. Coniglione¹³, P. Coyle⁸, A. Creusot⁹, A. F. Díaz²³, G. de Wasseige⁹, A. Deschamps²⁴, C. Distefano¹³, I. Di Palma^{18,19}, A. Domi^{15,17}, C. Donzaud^{9,25}, D. Dornic⁸, D. Drouhin^{1,2}, T. Eberl⁶, T. van Eeden¹⁵, D. van Eijk¹⁵, N. El Khayati¹², A. Enzenhöfer⁸, P. Fermani^{18,19}, G. Ferrara¹³, F. Filippini^{21,26}, L.A. Fusco⁸, Y. Gatelet⁹, P. Gay^{27,9}, H. Glotin²⁸, R. Gozzini³, R. Gracia Ruiz¹⁵, K. Graf⁶, C. Guidi^{5,29}, S. Hallmann⁶, H. van Haren³⁰, A.J. Heijboer¹⁵, Y. Hello²⁴, J.J. Hernández-Rey³, J. Höfl⁶, J. Hofestädt⁶, F. Huang⁸, G. Illuminati^{9,21,26}, C.W. James³¹, B. Jisse-Jung¹⁵, M. de Jong^{15,32}, P. de Jong¹⁵, M. Kadler³³, O. Kalekin⁶, U. Katz⁶, N.R. Khan-Chowdhury³, A. Kouchner⁹, I. Kreykenbohm³⁴, V. Kulikovskiy^{5,36}, R. Lahmann⁶, R. Le Breton⁹, D. Lefèvre³⁵, E. Leonora³⁶, G. Levi^{21,26}, M. Lincetto⁸, D. Lopez-Coto³⁷, S. Loucatos^{38,9}, L. Maderer⁹, J. Manczak³, M. Marcelin¹⁰, A. Margiotta^{21,26}, A. Marinelli³⁹, J.A. Martínez-Mora⁷, K. Melis^{15,17}, P. Migliozzi³⁹, A. Moussa¹⁴, R. Müller¹⁵, L. Nauta¹⁵, S. Navas³⁷, E. Nezri¹⁰, B. O'Fearraigh¹⁵, A. Păun¹⁶, G.E. Păvălaș¹⁶, C. Pellegrino^{21,40,41}, M. Perrin-Terrin⁸, V. Pestel¹⁵, P. Piattelli¹³, C. Pieterse³, C. Poirè⁷, V. Popa¹⁶, T. Pradier¹, N. Randazzo³⁶, S. Reck⁶, G. Riccobene¹³, A. Romanov^{5,29}, A. Sánchez-Losa^{3,22}, D. F. E. Samtleben^{15,32}, M. Sanguineti^{5,29}, P. Sapienza¹³, J. Schnabel⁶, J. Schumann⁶, F. Schüssler³⁸, M. Spurio^{21,26}, Th. Stolarczyk³⁸, M. Taiuti^{5,29}, Y. Tayalati¹², S.J. Tingay³¹, B. Vallage^{38,9}, V. Van Elewyck^{9,41}, F. Versari^{21,26,9}, S. Viola¹³, D. Vivolo^{39,43}, J. Wilms³⁴, S. Zavatarelli⁵, A. Zegarelli^{18,19}, J.D. Zornoza³, and J. Zúñiga³

¹Université de Strasbourg, CNRS, IPHC UMR 7178, F-67000 Strasbourg, France. ² Université de Haute Alsace, F-68100 Mulhouse, France. ³IFIC - Instituto de Física Corpuscular (CSIC - Universitat de València) c/ Catedrático José Beltrán, 2 E-46980 Paterna, Valencia, Spain. ⁴Technical University of Catalonia, Laboratory of Applied Bioacoustics, Rambla Exposició, 08800 Vilanova i la Geltrú, Barcelona, Spain. ⁵INFN - Sezione di Genova, Via Dodecaneso 33, 16146 Genova, Italy. ⁶Friedrich-Alexander-Universität Erlangen-Nürnberg, Erlangen Centre for Astroparticle Physics, Erwin-Rommel-Str. 1, 91058 Erlangen, Germany. ⁷Institut d'Investigació per a la Gestió Integrada de les Zones Costaneres (IGIC) - Universitat Politècnica de València. C/ Paranimf 1, 46730 Gandia, Spain. ⁸Aix Marseille Univ, CNRS/IN2P3, CPPM, Marseille, France. ⁹Université de Paris, CNRS, Astroparticule et Cosmologie, F-75013 Paris, France. ¹⁰Aix Marseille Univ, CNRS, CNES, LAM, Marseille, France. ¹¹National Center for Energy Sciences and Nuclear Techniques, B.P.1382, R. P.10001 Rabat, Morocco. ¹²University Mohammed V in Rabat, Faculty of Sciences, 4 av. Ibn Battouta, B.P. 1014, R.P. 10000 Rabat, Morocco. ¹³INFN - Laboratori Nazionali del Sud (LNS), Via S. Sofia 62, 95123 Catania, Italy. ¹⁴University Mohammed I, Laboratory of Physics of Matter and Radiations, B.P.717, Oujda 6000, Morocco. ¹⁵Nikhef, Science Park, Amsterdam, The Netherlands. ¹⁶Institute of Space Science, RO-077125 Bucharest, Măgurele, Romania. ¹⁷Universiteit van Amsterdam, Instituut voor Hoge-Energie Fysica, Science Park 105, 1098 XG Amsterdam, The Netherlands. ¹⁸INFN - Sezione di Roma, P.le Aldo Moro 2, 00185 Roma, Italy. ¹⁹Dipartimento di Fisica dell'Università La Sapienza, P.le Aldo Moro 2, 00185 Roma, Italy. ²⁰LPHEA, Faculty of Science - Semlali, Cadi Ayyad University, P.O.B. 2390, Marrakech, Morocco. ²¹INFN - Sezione di Bologna, Viale Berti-Pichat 6/2, 40127 Bologna, Italy. ²²INFN - Sezione di Bari, Via E. Orabona 4, 70126 Bari, Italy. ²³Department of Computer Architecture and Technology/CITIC, University of Granada, 18071 Granada, Spain. ²⁴Géoazur, UCA, CNRS, IRD, Observatoire de la Côte d'Azur, Sophia Antipolis, France. ²⁵Université Paris-Sud, 91405 Orsay Cedex, France. ²⁶Dipartimento di Fisica e Astronomia dell'Università, Viale Berti Pichat 6/2, 40127 Bologna, Italy. ²⁷Laboratoire de Physique Corpusculaire, Clermont Université, Université Blaise Pascal, CNRS/IN2P3, BP 10448, F-63000 Clermont-Ferrand, France. ²⁸LIS, UMR Université de Toulon, Aix Marseille Université, CNRS, 83041 Toulon, France. ²⁹Dipartimento di Fisica dell'Università, Via Dodecaneso 33, 16146 Genova, Italy. ³⁰Royal Netherlands Institute for Sea Research (NIOZ), Landsdiep 4, 1797 SZ 't Horntje (Texel), the Netherlands. ³¹International Centre for Radio Astronomy Research - Curtin University, Bentley, WA 6102, Australia. ³²Huygens-Kamerlingh Onnes Laboratorium, Universiteit Leiden, The Netherlands. ³³Institut für Theoretische Physik und Astrophysik, Universität Würzburg, Emil-Fischer Str. 31, 97074 Würzburg, Germany. ³⁴Dr. Reemis-Sternwarte and ECAP, Friedrich-Alexander-Universität Erlangen-Nürnberg, Sternwartstr. 7, 96049 Bamberg, Germany. ³⁵Mediterranean Institute of Oceanography (MIO), Aix-Marseille University, 13288, Marseille, Cedex 9, France; Université du Sud Toulon-Var, CNRS-INSU/IRD UMR 110, 83957, La Garde Cedex, France. ³⁶INFN - Sezione di Catania, Via S. Sofia 64, 95123 Catania, Italy. ³⁷Dpto. de Física Teórica y del Cosmos & C.A.F.P.E., University of Granada, 18071 Granada, Spain. ³⁸IRFU, CEA, Université Paris-Saclay, F-91191 Gif-sur-Yvette, France. ³⁹INFN - Sezione di Napoli, Via Cintia 80126 Napoli, Italy. ⁴⁰Museo Storico della Fisica e Centro Studi e Ricerche Enrico Fermi, Piazza del Viminale 1, 00184, Roma. ⁴¹INFN - CNAF, Viale C. Berti Pichat 6/2, 40127, Bologna. ⁴²Institut Universitaire de France, 75005 Paris, France. ⁴³Dipartimento di Fisica dell'Università Federico II di Napoli, Via Cintia 80126, Napoli, Italy.

Full Authors List: HAWC Collaboration

A.U. Abeysekara⁴⁸, A. Albert²¹, R. Alfaro¹⁴, C. Alvarez⁴¹, J.D. Álvarez⁴⁰, J.R. Angeles Camacho¹⁴, J.C. Arteaga-Velázquez⁴⁰, K. P. Arunbabu¹⁷, D. Avila Rojas¹⁴, H.A. Ayala Solares²⁸, R. Babu²⁵, V. Baghmany¹⁵, A.S. Barber⁴⁸, J. Becerra Gonzalez¹¹, E. Belmont-Moreno¹⁴, S.Y. BenZvi²⁹, D. Berley³⁹, C. Brisbois³⁹, K.S. Caballero-Mora⁴¹, T. Capistrán¹², A. Carramiñana¹⁸, S. Casanova¹⁵, O. Chaparro-Amaro³, U. Cotti⁴⁰, J. Cotzomi⁸, S. Coutiño de León¹⁸, E. De la Fuente⁴⁶, C. de León⁴⁰, L. Diaz-Cruz⁸, R. Diaz Hernandez¹⁸, J.C. Díaz-Vélez⁴⁶, B.L. Dingus²¹, M. Durocher²¹, M.A. DuVernois⁴⁵, R.W. Ellsworth³⁹, K. Engel³⁹, C. Espinoza¹⁴, K.L. Fan³⁹, K. Fang⁴⁵, M. Fernández Alonso²⁸, B. Fick²⁵, H. Fleischhack^{51,11,52}, J.L. Flores⁴⁶, N.I. Fraija¹², D. Garcia¹⁴, J.A. García-González²⁰, J. L. García-Luna⁴⁶, G. García-Torales⁴⁶, F. Garfias¹², G. Giacinti²², H. Goksu²², M.M. González¹², J.A. Goodman³⁹, J.P. Harding²¹, S. Hernandez¹⁴, I. Herzog²⁵, J. Hinton²², B. Hona⁴⁸, D. Huang²⁵, F. Hueyotl-Zahuantitla⁴¹, C.M. Hui²³, B. Humensky³⁹, P. Hütemeyer²⁵, A. Iriarte¹², A. Jardín-Blicq^{22,49,50}, H. Jhee⁴³, V. Joshi⁷, D. Kieda⁴⁸, G.J. Kunde²¹, S. Kunwar²², A. Lara¹⁷, J. Lee⁴³, W.H. Lee¹², D. Lennarz⁹, H. León Vargas¹⁴, J. Linnemann²⁴, A.L. Longinotti¹², R. López-Coto¹⁹, G. Luis-Raya⁴⁴, J. Lundeen²⁴, K. Malone²¹, V. Marandon²², O. Martínez⁸, I. Martínez-Castellanos³⁹, H. Martínez-Huerta³⁸, J. Martínez-Castro³, J.A.J. Matthews⁴², J. McEnery¹¹, P. Miranda-Romagnoli³⁴, J.A. Morales-Soto⁴⁰, E. Moreno⁸, M. Mostafá²⁸, A. Nayerhoda¹⁵, L. Nellen¹³, M. Newbold⁴⁸, M.U. Nisa²⁴, R. Noriega-Papaqui³⁴, L. Olivera-Nieto²², N. Omodei³², A. Peisker²⁴, Y. Pérez Araujo¹², E.G. Pérez-Pérez⁴⁴, C.D. Rho⁴³, C. Rivière³⁹, D. Rosa-Gonzalez¹⁸, E. Ruiz-Velasco²², J. Ryan²⁶, H. Salazar⁸, F. Salesa Greus^{15,53}, A. Sandoval¹⁴, M. Schneider³⁹, H. Schoorlemmer²², J. Serna-Franco¹⁴, G. Sinnis²¹, A.J. Smith³⁹, R.W. Springer⁴⁸, P. Surajbali²², I. Taboada⁹, M. Tanner²⁸, K. Tollefson²⁴, I. Torres¹⁸, R. Torres-Escobedo³⁰, R. Turner²⁵, F. Ureña-Mena¹⁸, L. Villaseñor⁸, X. Wang²⁵, I.J. Watson⁴³, T. Weisgarber⁴⁵, F. Werner²², E. Willcox³⁹, J. Wood²³, G.B. Yodh³⁵, A. Zepeda⁴, H. Zhou³⁰

¹Barnard College, New York, NY, USA, ²Department of Chemistry and Physics, California University of Pennsylvania, California, PA, USA, ³Centro de Investigación en Computación, Instituto Politécnico Nacional, Ciudad de México, México, ⁴Physics Department, Centro de Investigación y de Estudios Avanzados del IPN, Ciudad de México, México, ⁵Colorado State University, Physics Dept., Fort Collins, CO, USA, ⁶DCI-UDG, Leon, Gto, México, ⁷Erlangen Centre for Astroparticle Physics, Friedrich Alexander Universität, Erlangen, BY, Germany, ⁸Facultad de Ciencias Físico Matemáticas, Benemérita Universidad Autónoma de Puebla, Puebla, México, ⁹School of Physics and Center for Relativistic Astrophysics, Georgia Institute of Technology, Atlanta, GA, USA, ¹⁰School of Physics Astronomy and Computational Sciences, George Mason University, Fairfax, VA, USA, ¹¹NASA Goddard Space Flight Center, Greenbelt, MD, USA, ¹²Instituto de Astronomía, Universidad Nacional Autónoma de México, Ciudad de México, México, ¹³Instituto de Ciencias Nucleares, Universidad Nacional Autónoma de México, Ciudad de México, México, ¹⁴Instituto de Física, Universidad Nacional Autónoma de México, Ciudad de México, México, ¹⁵Institute of Nuclear Physics, Polish Academy of Sciences, Krakow, Poland, ¹⁶Instituto de Física de São Carlos, Universidade de São Paulo, São Carlos, SP, Brasil, ¹⁷Instituto de Geofísica, Universidad Nacional Autónoma de México, Ciudad de México, México, ¹⁸Instituto Nacional de Astrofísica, Óptica y Electrónica, Tonantzintla, Puebla, México, ¹⁹INFN Padova, Padova, Italy, ²⁰Tecnologico de Monterrey, Escuela de Ingeniería y Ciencias, Ave. Eugenio Garza Sada 2501, Monterrey, N.L., 64849, México, ²¹Physics Division, Los Alamos National Laboratory, Los Alamos, NM, USA, ²²Max-Planck Institute for Nuclear Physics, Heidelberg, Germany, ²³NASA Marshall Space Flight Center, Astrophysics Office, Huntsville, AL, USA, ²⁴Department of Physics and Astronomy, Michigan State University, East Lansing, MI, USA, ²⁵Department of Physics, Michigan Technological University, Houghton, MI, USA, ²⁶Space Science Center, University of New Hampshire, Durham, NH, USA, ²⁷The Ohio State University at Lima, Lima, OH, USA, ²⁸Department of Physics, Pennsylvania State University, University Park, PA, USA, ²⁹Department of Physics and Astronomy, University of Rochester, Rochester, NY, USA, ³⁰Tsung-Dao Lee Institute and School of Physics and Astronomy, Shanghai Jiao Tong University, Shanghai, China, ³¹Sungkyunkwan University, Gyeonggi, Rep. of Korea, ³²Stanford University, Stanford, CA, USA, ³³Department of Physics and Astronomy, University of Alabama, Tuscaloosa, AL, USA, ³⁴Universidad Autónoma del Estado de Hidalgo, Pachuca, Hgo., México, ³⁵Department of Physics and Astronomy, University of California, Irvine, Irvine, CA, USA, ³⁶Santa Cruz Institute for Particle Physics, University of California, Santa Cruz, Santa Cruz, CA, USA, ³⁷Universidad de Costa Rica, San José, Costa Rica, ³⁸Department of Physics and Mathematics, Universidad de Monterrey, San Pedro Garza García, N.L., México, ³⁹Department of Physics, University of Maryland, College Park, MD, USA, ⁴⁰Instituto de Física y Matemáticas, Universidad Michoacana de San Nicolás de Hidalgo, Morelia, Michoacán, México, ⁴¹FCFM-MCTP, Universidad Autónoma de Chiapas, Tuxtla Gutiérrez, Chiapas, México, ⁴²Department of Physics and Astronomy, University of New Mexico, Albuquerque, NM, USA, ⁴³University of Seoul, Seoul, Rep. of Korea, ⁴⁴Universidad Politécnica de Pachuca, Pachuca, Hgo, México, ⁴⁵Department of Physics, University of Wisconsin-Madison, Madison, WI, USA, ⁴⁶CUCEI, CUCEA, Universidad de Guadalajara, Guadalajara, Jalisco, México, ⁴⁷Universität Würzburg, Institute for Theoretical Physics and Astrophysics, Würzburg, Germany, ⁴⁸Department of Physics and Astronomy, University of Utah, Salt Lake City, UT, USA, ⁴⁹Department of Physics, Faculty of Science, Chulalongkorn University, Pathumwan, Bangkok 10330, Thailand, ⁵⁰National Astronomical Research Institute of Thailand (Public Organization), Don Kaeo, MaeRim, Chiang Mai 50180, Thailand, ⁵¹Department of Physics, Catholic University of America, Washington, DC, USA, ⁵²Center for Research and Exploration in Space Science and Technology, NASA/GSFC, Greenbelt, MD, USA, ⁵³Instituto de Física Corpuscular, CSIC, Universitat de València, Paterna, Valencia, Spain